Stability analysis of networked and quantized linear control systems[☆]

S.J.L.M. van Loon [*], M.C.F. Donkers, N. van de Wouw, W.P.M.H. Heemels

Eindhoven University of Technology, Department of Mechanical Engineering, 5600 MB Eindhoven, The Netherlands

ABSTRACT

The presence of a communication network in a control loop induces imperfections, such as quantization effects, packet dropouts, time-varying transmission intervals, time-varying transmission delays and communication constraints. The objectives of this paper are to provide a unifying modeling framework that incorporates all these imperfections simultaneously, and to present novel techniques for the stability analysis for these networked control systems (NCSs). In contrast to many other papers that consider quantization in NCSs, we incorporate quantization effects in the modeling framework by modeling them as norm-bounded additive disturbances on both plant and controller signals. We focus on linear plants and controllers, and periodic and quadratic protocols, which leads to a modeling framework for NCSs based on discrete-time switched linear uncertain systems. Using an overapproximated system in the form of a polytopic model with additive norm-bounded uncertainty, we propose LMI-based techniques to analyze the input-to-state stability (ISS) and the ℓ_2-gain properties of the obtained NCS models with respect to the norm-bounded additive disturbances induced by quantization. These ISS and ℓ_2-gain conditions will be used to assess closed-loop stability and performance for two classes of quantizers. We illustrate the effectiveness of the developed theory on a benchmark example of a batch reactor.

© 2013 Elsevier Ltd. All rights reserved.

1. Introduction

Networked control systems (NCSs) are feedback control systems, in which the control loops are closed over a shared communication network. Compared to a traditional control system, in which the sensors, controllers and actuators are connected through dedicated point-to-point connections, NCSs offer advantages, such as, e.g., increased flexibility and maintainability of the system, and reduced wiring. However, NCSs also introduce new challenges that need to be overcome before the advantages they offer can be fully exploited. Generally speaking, NCSs are subject to network-induced communication imperfections and constraints that can be categorized into five types: (i) quantization errors, (ii) packet dropouts, (iii) time-varying sampling/transmission intervals, (iv) time-varying transmission delays and (v) communication constraints. All these networked-induced imperfections may degrade the closed-loop performance of an NCS, or even worse, may cause instability. Therefore, it is important to investigate how these effects influence closed-loop stability of the NCS. Because in any NCS, all the previously mentioned imperfections are present simultaneously, it is important to develop

---

a comprehensive framework that allows to study the joint presence of all the network-induced effects. Namely, such a framework allows to make design tradeoffs between control properties, such as stability and performance, and network-related properties such as delays, scheduling, bandwidth limitations etc. Nevertheless, most of the available literature on NCS considers only some of the network-induced phenomena.

For instance, [1–3] consider (iii)–(v) simultaneously, [4] focuses on type (i), (ii) and (iv) phenomena, [5] considers (ii) and (v), [6–9] study (iii) and (iv), [10] considers (ii) and (iv), [11] focuses on (ii) and (iii), where [12,13] study (ii)–(iv), and [14] considers (i), (iii) and (v). Up to now, the only result that considers all these imperfections simultaneously, although under some restrictions, is [15].

To study the impact of these networked-induced phenomena on the stability and performance of NCSs, several models have been developed. Roughly speaking, three different approaches towards modeling and stability analysis have been considered in the literature, i.e., an approach based on discrete-time parameter varying systems, see, e.g., [2,7,9,13,12], a continuous-time approach based on impulsive or jump-flow systems, see, e.g., [3,14,15] and an approach based on delayed (impulsive) differential equations, see, e.g., [4,8,9,16].

In this paper, we focus on linear plants and controllers and study the stability of the corresponding NCSs in the presence of (i), (iii)–(v) types of network-induced phenomena. The type (ii) network-induced phenomenon, i.e., packet dropouts, can also be accommodated for by modeling them as prolongation of the transmission interval, see Remark 3. In fact, this paper generalizes the work of [2] by including quantization, which requires different techniques to analyze the closed-loop stability and performance, as we will show below. As already mentioned, the only other result in the literature that can study all networked-induced phenomena simultaneously is [15]. The difference between [15] and the work presented in this paper is that [15] use a modeling framework based on impulsive systems, while we take an approach based on discrete-time switched linear uncertain systems. As was shown in [2], the latter approach can lead to less conservative results (e.g., in terms of allowable bounds on delays and sampling intervals), in the linear context, and allows the controller to be given in continuous-time as well as in discrete-time. We note that discrete-time controllers are particularly relevant as NCSs are inherently digital. These aspects strongly motivate the generalization of [2], leading to a unifying framework for NCSs including all five mentioned network-induced imperfections.

The increasing interest in NCSs stimulates the research on quantized feedback control in general, see, e.g., the overview paper [17], since one of the limiting factors in an NCS is the finite capacity of the communication channel. Therefore, a significant amount of research has been devoted to the problem of determining the minimum bit rate that is required to stabilize a (non)linear system through feedback over a finite-bandwidth communication channel, see, e.g., [18–22], and references therein. Whereas these works are entirely devoted on the aspect of quantization, we focus in this paper on incorporating quantization-induced disturbances as one of the stability and performance limiting factors in a comprehensive modeling and analysis framework for NCSs, while also including the other networked-induced imperfections and allow for dynamic output-feedback controllers. In doing so, we focus on two of the most common types of memoryless quantizers treated in the NCS literature, being, uniform quantizers, see, e.g., [23], and logarithmic quantizers, see, e.g., [19–21]. In addition, we also comment on how 'zoom' quantizers, see, e.g., [18], could be analyzed as well in Remark 5.

Besides quantization, we also consider so-called communication constraints, which are a result of the fact that the communication network is typically shared by multiple (actuator and sensor) nodes, and only one node can access the network at a given time instant. Therefore, scheduling protocols are needed that determine when a certain node is allowed to access the network. We provide techniques for assessing stability of the NCS for two classes of protocols, namely, quadratic and periodic protocols. The two well-known Try-Once-Discard (TOD) and the Round-Robin (RR) protocols are special cases of these two classes. Finally, we include the uncertainties induced by time-varying delays and transmission intervals within the discrete-time modeling framework employed here, which leads to discrete-time switched linear system models with exponential uncertainty. To properly handle this exponential uncertainty, we extend the overapproximation technique described in [2] to arrive at a discrete-time polytopic model with additive norm-bounded uncertainty that is subject to an additive disturbance (due to quantization). Using this overapproximated system, we can guarantee input-to-state stability (ISS) and a certain ℓ_2-gain using newly developed conditions based on LMIs. Using these notions of ISS and ℓ_2-gain, we can assess closed-loop stability and performance of the NCS.

The remainder of this paper is organized as follows. After introducing the necessary notational conventions, we introduce the model of the NCS in Section 2 and propose a method to formulate it as a discrete-time switched linear system that is subject to a quantization-induced disturbance. In this section, we also introduce the classes of protocols and the types of (memoryless) quantizers considered in this paper. Furthermore, we give a precise problem formulation. Subsequently, in Section 3, we formalize a procedure to overapproximate the NCS model by a polytopic system with additive norm-bounded uncertainty, by extending the procedure given in [2]. In Section 4, we provide conditions for ISS and the ℓ_2-gain of the NCS in terms of LMIs. How these conditions can be used to guarantee stability of the overall NCS for two quantizers will be discussed in Section 5. Finally, we illustrate the theoretical results using a numerical benchmark example in Section 6 and draw conclusions in Section 7. The Appendix contains the proofs of the more technical results.

1.1. Nomenclature

The following notational conventions will be used. Let $\mathbb{Z}$, $\mathbb{N}$, $\mathbb{R}$, $\mathbb{R}_{\geq 0}$ denote the set of integers, non-negative integers, real numbers and nonnegative real numbers, respectively. A block-diagonal matrix is denoted as $\mathrm{diag}(A_1, \ldots, A_n)$ with the
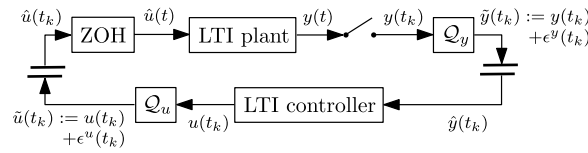
Fig. 1. Schematic overview of the NCS.

entries $A_1, \ldots, A_n$ on the diagonal and $A^\top \in \mathbb{R}^{m \times n}$ denotes the transposed of matrix $A \in \mathbb{R}^{n \times m}$. For a vector $x \in \mathbb{R}^n$, we denote by x^i the i-th component and $\|x\| := \sqrt{x^\top x} = \sqrt{\sum_i |x^i|^2}$ its Euclidean norm. For a symmetric matrix A, we denote $\lambda_{\max}(A)$, $\lambda_{\min}(A)$ as the maximum and minimum eigenvalue of A, respectively. We denote by $\|A\| := \sqrt{\lambda_{\max}(A^\top A)}$ the spectral norm of a matrix A. Furthermore, for a discrete-time signal $z : \mathbb{N} \to \mathbb{R}^n$, the ℓ_2-norm is defined as $\|z\|_{\ell_2} = \sqrt{\sum_{k=0}^{\infty} \|z_k\|^2}$ and the ℓ_∞-norm as $\|z\|_{\ell_\infty} = \sup_{k \in \mathbb{N}} \|z_k\|$. Furthermore, we define the sets of signals with a finite ℓ_2 or ℓ_∞-norm as $\ell_p := \{z : \mathbb{N} \to \mathbb{R}^n \mid \|z\|_{\ell_p} < \infty\}$ for $p = \{2, \infty\}$, respectively. We sometimes write symmetric matrices of the form $\begin{bmatrix} A & B \\ B^\top & C \end{bmatrix}$, as $\begin{bmatrix} A & B \\ \star & C \end{bmatrix}$. The convex hull and interior of a set $\mathcal{A}$ are denoted by co$\mathcal{A}$ and int$\mathcal{A}$, respectively.

2. NCS model and problem statement

In this section, we introduce the model describing NCSs subject to quantization, communication constraints (protocols), varying transmission intervals and delays. We will later comment on how dropouts can be included as well (see Remark 3 below). The NCS that we consider in this paper is schematically depicted in Fig. 1, where ZOH denotes a zero-order hold function that transforms the discrete-time control input $\hat{u}(t_k)$ to a continuous-time control input $\hat{u}(t)$, and $\mathcal{Q}_y$ and $\mathcal{Q}_u$ represent the quantizers. The plant is given by a linear time-invariant (LTI) continuous-time model of the form

$$\begin{cases} \dfrac{\mathrm{d}}{\mathrm{d}t} x^p(t) = A^p x^p(t) + B^p \hat{u}(t) \\ y(t) = C^p x^p(t), \end{cases} \tag{1}$$

where $x^p \in \mathbb{R}^{n_p}$ denotes the state of the plant, $\hat{u} \in \mathbb{R}^{n_u}$ the control variable available at the actuator, $y \in \mathbb{R}^{n_y}$ the (measured) output of the plant and $t \in \mathbb{R}_{\geqslant 0}$ the time. The LTI controller is assumed to be given in discrete-time by

$$\begin{cases} x^c_{k+1} = A^c x^c_k + B^c \hat{y}_k \\ u(t_k) = C^c x^c_k + D^c \hat{y}(t_k), \end{cases} \tag{2}$$

where $x^c \in \mathbb{R}^{n_c}$ denotes the state of the controller, $\hat{y} \in \mathbb{R}^{n_y}$ a 'networked' version of the output of the plant available at the controller, $u \in \mathbb{R}^{n_u}$ denotes the controller output and t_k are the transmission instants. The 'networked' signals $\hat{y} : \mathbb{R}_{\geqslant 0} \to \mathbb{R}^{n_y}$ and $\hat{u} : \mathbb{R}_{\geqslant 0} \to \mathbb{R}^{n_u}$ will be taken left-continuous, meaning that $\lim_{t \uparrow s} \hat{y}(t) = \hat{y}(s)$ and $\lim_{t \uparrow s} \hat{u}(t) = \hat{u}(s)$ for all $s \in \mathbb{R}_{\geqslant 0}$. At transmission instant t_k, $k \in \mathbb{N}$, (parts of) the outputs of the plant $y(t_k)$ and controller $u(t_k)$ are sampled and quantized, after which they are transmitted over the network. We assume that this data arrives after a delay τ_k at instant $r_k := t_k + \tau_k$, called the arrival instant. This is illustrated in Fig. 2. The states of the controller x^c_{k+1} are updated after the most recently received output of the plant $\hat{y}$ is updated, i.e., by using $\hat{y}_k := \lim_{t \downarrow r_k} \hat{y}(t)$. Note that, this update of x^c_{k+1} has to be performed in the time interval $(r_k, t_{k+1}]$.

Remark 1. Note that, although we only consider a discrete-time controller in (2), the framework as presented in this paper also allows the controller to be given in continuous-time, see Remark 4 below.

Let us now explain in more detail the consequences of sampling, delays, zero-order hold, quantization and communication constraints. To do so, let us consider the case where the plant is equipped with n_y sensors and n_u actuators that are grouped into N nodes. At each transmission instant t_k, $k \in \mathbb{N}$, one node, denoted by $\sigma_k \in \{1, \ldots, N\}$, gets access to the network and transmits its current values. These transmitted values are received and implemented on the controller or the plant at arrival instant r_k. The sensor(s)/actuator(s), corresponding to the node that is allowed access to the network, collect their values from a sampled and quantized measurement of the corresponding entries of $y(t_k)$ and $u(t_k)$. This quantization process introduces a so-called quantization-induced error in both $y(t_k)$ and $u(t_k)$, denoted by $\epsilon^y(t_k)$ and $\epsilon^u(t_k)$, respectively, which are also illustrated in Figs. 1 and 2. The quantized signals are denoted by $\tilde{y}(t_k) = y(t_k) + \epsilon^y(t_k)$ and $\tilde{u}(t_k) = u(t_k) + \epsilon^u(t_k)$. We will make the quantization-induced error precise for two types of quantizers below. Furthermore, we assume that a transmission only occurs after the previous transmission has arrived, i.e., $t_{k+1} > r_k \geqslant t_k$, for all $k \in \mathbb{N}$. In other words, we consider the case where the transmission delays are smaller than the transmission interval, i.e., $\tau_k < h_k$ for all $k \in \mathbb{N}$. After each transmission and reception, the values in $\hat{y}$ and $\hat{u}$ are updated with the latest received data, while the
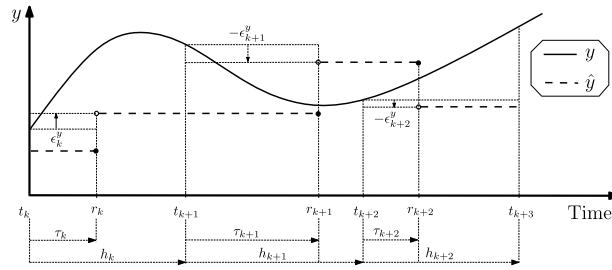
Fig. 2. Illustration of a typical evolution of y and $\hat{y}$ for a quantized control system.

other values in $\hat{y}$ and $\hat{u}$ remain the same. This leads to the following constrained data exchange:

$$\begin{cases} \hat{y}(t) = \Gamma_{\sigma_k}^y (y(t_k) + \epsilon^y(t_k)) + (I - \Gamma_{\sigma_k}^y)\hat{y}(t_k) \\ \hat{u}(t) = \Gamma_{\sigma_k}^u (u(t_k) + \epsilon^u(t_k)) + (I - \Gamma_{\sigma_k}^u)\hat{u}(t_k) \end{cases} \tag{3}$$

for all $t \in (r_k, r_{k+1}]$, which models all the network effects, i.e., sampling, quantization, delays, scheduling and the zero-order hold. In (3), $\Gamma_{\sigma_i} := \mathrm{diag}(\Gamma_{\sigma_i}^y, \Gamma_{\sigma_i}^u), i = \{1, \ldots, N\}$, are diagonal matrices given by

$$\Gamma_i = \mathrm{diag}(\gamma_{i,1}, \ldots, \gamma_{i,n_y+n_u}). \tag{4}$$

In (4), the elements $\gamma_{i,j}$, with $i \in \{1, \ldots, N\}$ and $j \in \{1, \ldots, n_y\}$, are equal to one, if plant output y^j is in node i and are zero elsewhere, and elements $\gamma_{i,j+n_y}$, with $i \in \{1, \ldots, N\}$ and $j \in \{1, \ldots, n_u\}$, are equal to one, if the controller output u^j is in node i and are zero elsewhere.

Remark 2. For the sake of generality, we allow both sensors and actuators to be assigned to the same node. However, in practice, this will rarely be the case and a node will typically contain either sensors or actuators.

The value of $\sigma_k \in \{1, \ldots, N\}$ in (3) indicates which node is given access to the network at transmission instant $t_k, k \in \mathbb{N}$. Indeed, (3) reflects that the values in $\hat{y}$ and $\hat{u}$ are updated just after r_k, with the corresponding transmitted values at time t_k, while the others remain unaltered. A scheduling protocol determines the sequence $(\sigma_0, \sigma_1, \ldots)$ and particular classes of protocols will be introduced in Section 2.2.

In this paper, we consider the case where both the transmission intervals $h_k := t_{k+1} - t_k, k \in \mathbb{N}$, as well as the transmission delays $\tau_k := r_k - t_k, k \in \mathbb{N}$, are time-varying, as also indicated in Fig. 2. We assume that the variations in the transmission intervals and delays are bounded and contained in the sets $[\underline{h}, \overline{h}]$ and $[\underline{\tau}, \overline{\tau}]$, respectively, with $0 < \underline{h} \leqslant \overline{h}$ and $0 \leqslant \underline{\tau} \leqslant \overline{\tau}$. Since we assume that the transmission delays are smaller than the transmission interval, we have that $(h_k, \tau_k) \in \Theta$, for all $k \in \mathbb{N}$, where

$$\Theta := \{(h, \tau) \in \mathbb{R}^2 \mid h \in [\underline{h}, \overline{h}], \ \tau \in [\underline{\tau}, \min\{h, \overline{\tau}\})\}. \tag{5}$$

Remark 3. The inclusion of packet dropouts can be realized by modeling them as prolongations of the transmission interval, see e.g., [2,3]. To do so, let us assume that there is a bound $\delta_d \in \mathbb{N}$ on the maximum number of successive packet dropouts. The stability bounds derived below are then still valid for $(h_k, \tau_k) \in \Theta'$, for all $k \in \mathbb{N}$, where

$$\Theta' := \{(h, \tau) \in \mathbb{R}^2 \mid h \in [\underline{h}, \overline{h}'], \ \tau \in [\underline{\tau}, \min\{h, \overline{\tau}\})\} \tag{6}$$

in which $\overline{h}' := \frac{\overline{h}}{\delta_d+1}$.

2.1. The NCS as a time-varying switched system

In this paper, we take a discrete-time modeling approach, and to derive a discrete-time model description, we first define the errors induced by the communication network and the quantizer as

$$\begin{cases} e^y(t) := \hat{y}(t) - y(t) \\ e^u(t) := \hat{u}(t) - u(t), \end{cases} \tag{7}$$

for all $t \in \mathbb{R}_{\geqslant 0}$. The discrete-time switched uncertain system can now be obtained by describing the evolution of the states between t_k and $t_{k+1} = t_k + h_k$. To do so, we define $x_k^p := x^p(t_k), y_k := y(t_k), u_k := u(t_k), \tilde{y}_k := \tilde{y}(t_k), \tilde{u}_k := \tilde{u}(t_k),$ $\hat{y}_k := \lim_{t \downarrow r_k} \hat{y}(t), \hat{u}_k := \lim_{t \downarrow r_k} \hat{u}(t), e_k^y := e^y(t_k), e_k^u := e^u(t_k), \epsilon_k^y := \epsilon^y(t_k)$ and $\epsilon_k^u := \epsilon^u(t_k)$. Since both $\hat{y}$ and $\hat{u}$, as in (3), are left-continuous piecewise constant signals, we can write $\hat{y}_{k-1} = \lim_{t \downarrow r_{k-1}} \hat{y}(t) = \hat{y}(r_k) = \hat{y}(t_k)$ and

$\hat{u}_{k-1} = \lim_{t \downarrow r_{k-1}} \hat{u}(t) = \hat{u}(r_k) = \hat{u}(t_k)$. As (3) and (7) yield $\hat{u}_{k-1} = u_k + e_k^u$ and $\hat{u}_k - \hat{u}_{k-1} = \Gamma_{\sigma_k}^u(\epsilon_k^u - e_k^u)$, we can write the exact discretization of (1) as follows:

$$x_{k+1}^p = e^{A^p h_k} x_k^p + \int_0^{h_k} e^{A^p s} ds B^p (u_k + e_k^u) + \int_0^{h_k - \tau_k} e^{A^p s} ds B^p \Gamma_{\sigma_k}^u (\epsilon_k^u - e_k^u). \tag{8}$$

The complete NCS model is obtained by combining (3), (7) and (8) and introducing

$$\bar{x}_k := \begin{bmatrix} x_k^{p\top} x_k^{c\top} & e_k^{y\top} & e_k^{u\top} \end{bmatrix}^\top, \qquad \bar{\epsilon}_k := \begin{bmatrix} \epsilon_k^{y\top} & \epsilon_k^{u\top} \end{bmatrix}^\top, \qquad \bar{z}_k := \begin{bmatrix} y_k^\top u_k^\top \end{bmatrix}^\top, \tag{9}$$

which results in the following discrete-time model;

$$\begin{cases} \bar{x}_{k+1} = \underbrace{\begin{bmatrix} A_{h_k} + E_{h_k} BDC & E_{h_k} BD - E_{h_k - \tau_k} B\Gamma_{\sigma_k} \\ C(I - A_{h_k} - E_{h_k} BDC) & I - D^{-1}\Gamma_{\sigma_k} + C(E_{h_k - \tau_k} B\Gamma_{\sigma_k} - E_{h_k} BD) \end{bmatrix}}_{=:\tilde{A}_{\sigma_k, h_k, \tau_k}} \bar{x}_k + \underbrace{\begin{bmatrix} E_{h_k - \tau_k} B\Gamma_{\sigma_k} \\ D^{-1}\Gamma_{\sigma_k} - CE_{h_k - \tau_k} B\Gamma_{\sigma_k} \end{bmatrix}}_{=:\tilde{B}_{\sigma_k, h_k, \tau_k}} \bar{\epsilon}_k \\ \bar{z}_k = \underbrace{\begin{bmatrix} DC & I - D^{-1} \end{bmatrix}}_{=:\tilde{H}_{\sigma_k}} \bar{x}_k \end{cases} \tag{10}$$

in which $\tilde{A}_{\sigma_k, h_k, \tau_k} \in \mathbb{R}^{n_x \times n_x}, \tilde{B}_{\sigma_k, h_k, \tau_k} \in \mathbb{R}^{n_x \times n_z}, \tilde{H}_{\sigma_k} \in \mathbb{R}^{n_z \times n_x}$, with $n_x := n_p + n_c + n_y + n_u, n_z := n_y + n_u$ and

$$A_\rho := \text{diag}(e^{A^p \rho}, A^c), \qquad B := \begin{bmatrix} 0 & B^p \\ B^c & 0 \end{bmatrix}, \qquad C := \text{diag}(C^p, C^c), \qquad D := \begin{bmatrix} I & 0 \\ D^c I \end{bmatrix},$$

$$E_\rho := \text{diag}\left(\int_0^\rho e^{A^p s} ds, I\right), \quad \rho \in \mathbb{R}. \tag{11}$$

Remark 4. In this paper, we consider the case where the controller is given in discrete-time, see (2). However, the type of model (10) also allows the controller to be given in continuous-time, as was shown in [2] for the case without quantization. In principle, this only requires the usage of different matrices (11) in (10), as provided in [2].

2.2. Protocols as switching functions

Based on the previous modeling steps, the NCS is described by a parameter-varying discrete-time switched linear system (10) that is subject to an unknown disturbance $\bar{\epsilon}$ induced by quantization. In this framework, scheduling protocols are considered as switching functions determining σ_k for each $k \in \mathbb{N}$. We consider two classes of protocols in this paper that have been introduced in [2], namely the class of quadratic and periodic protocols. In fact, we make a slight extension to the class of quadratic protocols. Furthermore, note that two well-known protocols, namely, the Try-Once-Discard (TOD) protocol and the Round-Robin (RR) protocol, see, e.g., [3,24], are special cases of these two protocol classes.

2.2.1. Quadratic protocols
In this paper, we consider quadratic protocols for which the switching function can be written as

$$\sigma_k = \min \left\{ \arg \min_{i \in \{1, \dots, N\}} \begin{bmatrix} \bar{x}_k \\ \bar{\epsilon}_k \end{bmatrix}^\top Q_i \begin{bmatrix} \bar{x}_k \\ \bar{\epsilon}_k \end{bmatrix} \right\}, \tag{12}$$

in which

$$Q_i = \begin{bmatrix} Q_{11}^i & Q_{12}^i \\ \star & Q_{22}^i \end{bmatrix}, \tag{13}$$

with certain given matrices $Q_{11}^i \in \mathbb{R}^{n_x \times n_x}$, $Q_{12}^i \in \mathbb{R}^{n_x \times n_z}$ and $Q_{22}^i \in \mathbb{R}^{n_z \times n_z}$, with $i \in \{1, \dots, N\}$. In the case multiple $\begin{bmatrix} \bar{x}_k \\ \bar{\epsilon}_k \end{bmatrix}^\top Q_i \begin{bmatrix} \bar{x}_k \\ \bar{\epsilon}_k \end{bmatrix}$ have the same smallest value, the node with the smallest $i \in \{1, \dots, N\}$, is given access to the network. The well-known TOD protocol belongs to this class of protocols. In the TOD protocol, the node that has the largest network-induced error, i.e., the largest difference between the most recently received values and the current quantized values of the signals corresponding to the node, given by $\hat{y}_{k-1} - \tilde{y}_k = (e_k^y + y_k) - (y_k + \epsilon_k^y)$ or $\hat{u}_{k-1} - \tilde{u}_k = (e_k^u + u_k) - (u_k + \epsilon_k^u), k \in \mathbb{N}$, is granted access to the network.[1] Hence, this network-induced error consists of the error induced by the communication network only and is given by

$$\tilde{e}_k := \begin{bmatrix} (\bar{e}_k^1 - \bar{\epsilon}_k^1)^\top, \dots, (\bar{e}_k^N - \bar{\epsilon}_k^N)^\top \end{bmatrix}^\top, \tag{14}$$

---

[1] Note that our formulation of the TOD protocol differs from the general framework presented in [14], as they use the difference between the exact current data and the already received data. However, in any practical setting, the only data that is available for any scheduling protocol is the current quantized data and the already received data.

in which $\bar{e}_k := [e_k^{y\top} \ e_k^{u\top}]^\top$. By defining $\hat{e}_k^i := \Gamma_i \tilde{e}_k$, where $\Gamma_i, i \in \{1, \ldots, N\}$, is given by (4), the TOD protocol, as introduced in [24], is given by

$$
\sigma_k = \min\left\{\arg\max_{i\in\{1,\ldots,N\}}\{\|\hat{e}_k^i\|\}\right\} = \min\left\{\arg\min_{i\in\{1,\ldots,N\}}\{-\tilde{e}_k^\top \Gamma_i \tilde{e}_k\}\right\}
$$

$$
= \min\left\{\arg\min_{i\in\{1,\ldots,N\}}\left\{-\begin{bmatrix}\hat{y}_{k-1} - \tilde{y}_k \\ \hat{u}_{k-1} - \tilde{u}_k\end{bmatrix}^\top \Gamma_i \begin{bmatrix}\hat{y}_{k-1} - \tilde{y}_k \\ \hat{u}_{k-1} - \tilde{u}_k\end{bmatrix}\right\}\right\}. \tag{15}
$$

Hence, the TOD protocol can be modeled as in (12) by adopting the following structure in the Q_i matrices:

$$
Q_i = \left[\begin{array}{cc|c} 0 & 0 & 0 \\ 0 & -\Gamma_i & \Gamma_i \\ 0 & \Gamma_i & -\Gamma_i \end{array}\right], \quad i \in \{1, \ldots, N\}. \tag{16}
$$

2.2.2. Periodic protocols

Another class of protocols that is considered in this paper is the class of so-called periodic protocols. A periodic protocol is a protocol that satisfies for some $\tilde{N} \in \mathbb{N}$

$$
\sigma_{k+\tilde{N}} = \sigma_k, \quad \text{for all } k \in \mathbb{N}. \tag{17}
$$

$\tilde{N}$ is then called the period of the protocol. Actually, the well-known RR protocol belongs to this class and is defined by

$$
\{\sigma_1, \ldots, \sigma_N\} = \{1, 2, \ldots, N\}, \tag{18}
$$

and period $\tilde{N} = N$, i.e., during each period of the protocol every node has access to the network exactly once and in a fixed sequence.

2.3. Quantization

As mentioned before, the quantizer introduces a quantization-induced error $\bar{\epsilon}$ that can be considered as a disturbance in the NCS model (10). In this paper, we assume that each plant output and control input is quantized separately according to the mapping $q^i : \mathbb{R} \rightarrow \mathcal{Q}^i, i \in \{1, \ldots, n_z\}$, in which $\mathcal{Q}^i$ is a finite or countable subset of $\mathbb{R}$. We consider two types of quantizers in this paper, which are discussed next (and we briefly comment on how another type of quantizer could be incorporated as well, see Remark 5).

2.3.1. Uniform quantizer

The uniform quantizer is defined by

$$
q^i(\bar{z}_k^i) = \zeta_i \left\lfloor \frac{\bar{z}_k^i}{\zeta_i} \right\rceil, \tag{19}
$$

where $\zeta_i > 0, i \in \{1, \ldots, n_z\}$ denotes the step size and $\lfloor \cdot \rceil : \mathbb{R} \rightarrow \mathbb{Z}$ is the rounding function that rounds off towards the nearest integer. In the case $\frac{\bar{z}_k^i}{\zeta_i}$ in (19) is exactly in between two integers, its value is rounded up towards the nearest positive integer if $\frac{\bar{z}_k^i}{\zeta_i} > 0$, and is rounded down towards the nearest negative integer if $\frac{\bar{z}_k^i}{\zeta_i} < 0$. This quantizer results in a quantization error for each input/output signal $\bar{z}_k^i, i \in \{1, \ldots, n_z\}$, satisfying

$$
|\bar{\epsilon}_k^i| = |\bar{z}_k^i - q^i(\bar{z}_k^i)| \leqslant \frac{\zeta_i}{2} \tag{20}
$$

for all $k \in \mathbb{N}$. Note that this type of quantizers introduces a bounded and nonvanishing quantization error, which prohibits asymptotic stabilization of the NCS. However, we can provide conditions that will guarantee the solutions to remain bounded and to converge to a vicinity of the origin. Hence, instead of asymptotic stability, only practical stability of the NCS can be achieved.

2.3.2. Logarithmic quantizer

A quantizer is called logarithmic if the quantization levels are linear on a logarithmic scale [19,20], i.e., the set of quantized levels is described by

$$
\mathcal{Q}^i = \{\pm w_j \mid w_j = \eta_i^j w_0^i, j \in \mathbb{Z}\} \cup \{0\}, \tag{21}
$$

for some $w_0^i > 0$ in which the quantization density per input/output signal is denoted by $\eta_i \in (0, 1), i \in \{1, \ldots, n_z\}$, see [19], where a small η_i corresponds to a course quantizer. According to [19,20], the associated quantizer is defined as

$$q^i(\bar{z}_k^i) = \begin{cases} w_j, & \text{if } \bar{z}_k^i \in \left(\dfrac{1}{1+\delta_i} w_j, \dfrac{1}{1-\delta_i} w_j \right] \text{ and } \bar{z}_k^i > 0; \\ -w_j, & \text{if } \bar{z}_k^i \in \left[\dfrac{-1}{1-\delta_i} w_j, \dfrac{-1}{1+\delta_i} w_j \right) \text{ and } \bar{z}_k^i < 0; \\ 0, & \text{if } \bar{z}_k^i = 0; \end{cases} \tag{22}$$

with $\delta_i = \frac{1-\eta_i}{1+\eta_i}$, $i \in \{1, \ldots, n_z\}$. For this type of quantizers, the quantization-induced error for each input/output signal $\bar{z}_k^i$, $i \in \{1, \ldots, n_z\}$, satisfies for $k \in \mathbb{N}$

$$|\bar{\epsilon}_k^i| = |\bar{z}_k^i - q(\bar{z}_k^i)| \leqslant \delta_i |\bar{z}_k^i|, \tag{23}$$

see [19,20]. Contrary to the uniform quantizer, the quantization error of the logarithmic quantizer does vanish as $\bar{z}_k \to 0$. Hence, for this type of quantizers, it is possible to provide conditions that guarantee asymptotic stability of the NCS.

2.4. Problem statement: input-to-state stability and ℓ_2-gain of the NCS

The problem studied in this paper is to analyze (practical) stability of the NCS given by (1)–(3) and (7), with protocols (12) or (17), and quantizers (19) or (22), where the time-varying and uncertain transmission intervals and transmission delays are taken from the set Θ defined in (5). The stability analysis will be based on studying (exponential) input-to-state stability (EISS) and the ℓ_2-gain properties of the system (10). We will show in Section 5 how these stability conditions guarantee (practical or exponential) stability for the corresponding NCSs with one of the two quantizers studied in this paper.

Let us now formally define the EISS and the ℓ_2-gain properties, in which we exploit the linearity properties of the closed-loop NCS model (10).

Definition 1 (*[25]*)**.** System (10) with switching sequences satisfying (12) or (17) is said to be exponentially input-to-state stable (EISS) with respect to $\bar{\epsilon} \in \ell_\infty$, if there exist $c \geqslant 0$, $\gamma_{\text{ISS}} > 0$ and $0 \leqslant \lambda < 1$ such that for any initial condition $\bar{x}_0 \in \mathbb{R}^{n_x}$, any sequence of transmission intervals $(h_0, h_1, \ldots)$, and any sequence of transmission delays $(\tau_0, \tau_1, \ldots)$, with $(h_k, \tau_k) \in \Theta$, for all $k \in \mathbb{N}$, it holds that

$$\|\bar{x}_k\| \leqslant c\lambda^k \|\bar{x}_0\| + \gamma_{\text{ISS}} \sup_{s \in [0, k-1]} \|\bar{\epsilon}_s\|. \tag{24}$$

Definition 2. System (10) with switching sequences satisfying (12) or (17) is said to have an ℓ_2-gain smaller than or equal to γ_{ℓ_2}, if there exist a function $\beta : \mathbb{R}_{\geqslant 0} \to \mathbb{R}_{\geqslant 0}$ such that for any $\bar{\epsilon} \in \ell_2$ and any initial condition $\bar{x}_0 \in \mathbb{R}^{n_x}$, any sequence of transmission intervals $(h_0, h_1, \ldots)$, and any sequence of transmission delays $(\tau_0, \tau_1, \ldots)$, with $(h_k, \tau_k) \in \Theta$, for all $k \in \mathbb{N}$, the corresponding output solution satisfies

$$\|\bar{z}\|_{\ell_2} \leqslant \beta_{\ell_2}(\|\bar{x}_0\|) + \gamma_{\ell_2} \|\bar{\epsilon}\|_{\ell_2}. \tag{25}$$

3. Obtaining a convex overapproximation

In the previous section, we obtained an NCS model in the form of a discrete-time switched uncertain linear system, as given by (10). However, the development of efficient stability analysis techniques for (10) directly is obstructed due to the fact that the uncertainties appear in an exponential fashion in both $\tilde{A}_{\sigma_k, h_k, \tau_k}$ and $\tilde{B}_{\sigma_k, h_k, \tau_k}$. Therefore, we apply a procedure that overapproximates system (10) by a polytopic system with a norm-bounded additive uncertainty of the form

$$\bar{x}_{k+1} = \left(\sum_{l=1}^{L} \alpha_k^l \bar{A}_{\sigma_k, l} + \bar{B} \Delta_k \bar{C}_{\sigma_k} \right) \bar{x}_k + \left(\sum_{l=1}^{L} \alpha_k^l \bar{E}_{\sigma_k, l} + \bar{B} \Delta_k \bar{F}_{\sigma_k} \right) \bar{\epsilon}_k \tag{26}$$

where $\bar{A}_{\sigma, l} \in \mathbb{R}^{n_x \times n_x}$, $\bar{B} \in \mathbb{R}^{n_x \times q}$, $\bar{C}_\sigma \in \mathbb{R}^{q \times n_x}$, $\bar{E}_{\sigma, l} \in \mathbb{R}^{n_x \times n_z}$, $\bar{F}_\sigma \in \mathbb{R}^{q \times n_z}$, for $\sigma \in \{1, \ldots, N\}$ and $l \in \{1, \ldots, L\}$, with L the number of vertices of the polytope. The vector $\alpha_k = [\alpha_k^1 \ \ldots \ \alpha_k^L]^\top \in \mathcal{A}$, $k \in \mathbb{N}$, is time varying with

$$\mathcal{A} = \left\{ \alpha \in \mathbb{R}^L | \sum_{l=1}^{L} \alpha^l = 1, \ \alpha^l \geqslant 0 \text{ for all } l \in \{1, \ldots, L\} \right\} \tag{27}$$

and $\Delta_k \in \boldsymbol{\Delta}$, $k \in \mathbb{N}$, where $\boldsymbol{\Delta}$ is a norm-bounded set of matrices in $\mathbb{R}^{q \times q}$ that describes the additive uncertainty. The system in (26) is an overapproximation of (10), in the sense that for all $\sigma \in \{1, \ldots, N\}$, it holds that

$$\left\{ \left[\tilde{A}_{\sigma, h, \tau} \ \ \tilde{B}_{\sigma, h, \tau} \right] \mid (h, \tau) \in \Theta \right\} \subseteq \left\{ \sum_{l=1}^{L} \alpha^l \left[\bar{A}_{\sigma, l} \ \ \bar{E}_{\sigma, l} \right] + \bar{B} \Delta \left[\bar{C}_\sigma \ \ \bar{F}_\sigma \right] \mid \alpha \in \mathcal{A}, \ \Delta \in \boldsymbol{\Delta} \right\}. \tag{28}$$

Overapproximating the uncertain system (10) by (26) in the sense of (28), is convenient for analysis, as obtaining EISS with a certain upper bound on the ISS-gain γ_{ISS}, and obtaining a certain upper bound on the ℓ_2-gain γ_{ℓ_2} of the system (26), imply that the system (10) is EISS with the same upper bound on the ISS-gain γ_{ISS} and has the same upper bound on the ℓ_2-gain γ_{ℓ_2} as well.

In this paper, we will employ an overapproximation technique based on gridding and norm-bounding, described in [2], to construct a polytopic system with a norm-bounded additive uncertainty of the form of (26), satisfying (28). In order to compute all individual matrices of (26), we slightly extended the procedure described in [2]. The extension lies in the construction of the matrices $\bar{E}_{\sigma,l}$ and $\bar{F}_\sigma$. Even though this extension is not major, it is necessary for enabling the analysis of quantization effects. For self-containedness, we provide a concise form of the extended algorithm below.

Procedure 1.

- Select distinct pairs $(\tilde{h}_l, \tilde{\tau}_l) \in \Theta, l \in \{1, \ldots, L\}$, called grid points, such that $\text{co}\mathcal{G} = \Theta$, where $\mathcal{G} = \cup_{l=1}^L \{(\tilde{h}_l, \tilde{\tau}_l)\}$. Furthermore, select a set of triangles $\mathcal{H} = \{\mathcal{S}_1, \ldots, \mathcal{S}_M\}$, with

$$\mathcal{S}_m = \text{co}\{(\tilde{h}_{l_1^m}, \tilde{\tau}_{l_1^m}), (\tilde{h}_{l_2^m}, \tilde{\tau}_{l_2^m}), (\tilde{h}_{l_3^m}, \tilde{\tau}_{l_3^m})\}, \tag{29}$$

where $l_j^m \in \{1, \ldots, L\}, j \in \{1, 2, 3\}$ for each $m \in \{1, \ldots, M\}$. Moreover, $\mathcal{H}$ forms a partitioning of Θ in the sense that $\bigcup_{m=1}^M \mathcal{S}_m = \Theta$ and for all $m, p \in \{1, \ldots, M\}$ and $p \neq m$, we have $\text{int}\mathcal{S}_p \cap \text{int}\mathcal{S}_m = \emptyset$, and $\text{int}\mathcal{S}_m \neq \emptyset$, for all $m \in \{1, \ldots, M\}$.
- Define $\bar{A}_{\sigma,l} := \tilde{A}_{\sigma,\tilde{h}_l,\tilde{\tau}_l}$ and $\bar{E}_{\sigma,l} := \tilde{B}_{\sigma,\tilde{h}_l,\tilde{\tau}_l}$, for all $\sigma \in \{1, \ldots, N\}$ and $(\tilde{h}_l, \tilde{\tau}_l) \in \mathcal{G}$.
- Construct the matrix $\bar{\Lambda} = \text{diag}(A^p, 0)$, and decompose it into its real Jordan form, i.e., $\bar{\Lambda} := T\Lambda T^{-1}$, where T is a transformation matrix and $\Lambda = \text{diag}(\Lambda_1, \ldots, \Lambda_K)$, with $\Lambda_i \in \mathbb{R}^{n_i \times n_i}, i \in \{1, \ldots, K\}$, the i-th real Jordan block of $\bar{\Lambda}$.
- Compute for each real Jordan block Λ_i the worst case approximation errors $\delta_i^A, \delta_i^{E_h}$ and $\delta_i^{E_{h-\tau}}, i \in \{1, \ldots, K\}$, of all triangles $\mathcal{S}_m \in \mathcal{H}, m \in \{1, \ldots, M\}$. For the sake of brevity, we refer to [2, Eq. (35) in Procedure III.1] for the exact definition of these approximation errors.
- Define

$$\bar{C}_\sigma := \begin{bmatrix} T^{-1} & 0 \\ T^{-1}BDC & T^{-1}BD \\ 0 & -T^{-1}B\Gamma_\sigma \end{bmatrix}, \qquad \bar{F}_\sigma := \begin{bmatrix} 0 \\ 0 \\ T^{-1}B\Gamma_\sigma \end{bmatrix},$$

and

$$\bar{B} := \begin{bmatrix} T & T & T \\ -CT & -CT & -CT \end{bmatrix} \cdot \text{diag}(\delta_1^A I_1, \ldots, \delta_K^A I_K, \delta_1^{E_h} I_1, \ldots, \delta_K^{E_h} I_K, \delta_1^{E_{h-\tau}} I_1, \ldots, \delta_K^{E_{h-\tau}} I_K), \tag{30}$$

with $I_i \in \mathbb{R}^{n_i \times n_i}$ an identity matrix of size complying with the i-th real Jordan block $\Lambda_i, i \in \{1, \ldots, K\}$.
- The additive uncertainty set $\boldsymbol{\Delta} \subseteq \mathbb{R}^{3(n_p+n_c) \times 3(n_p+n_c)}$ is now given by

$$\boldsymbol{\Delta} = \left\{ \text{diag}(\Delta^1, \ldots, \Delta^{3K}) \mid \Delta^{i+jK} \in \mathbb{R}^{n_i \times n_i}, \|\Delta^{i+jK}\| \leqslant 1, i \in \{1, \ldots, K\}, j \in \{0, 1, 2\} \right\}. \tag{31}$$

Although in this paper, we employ an overapproximation technique which is based on gridding and norm-bounding (GNB), all other existing techniques that embed the original model with the exponential uncertainties in a discrete-time polytopic model (with or without additive norm-bounded uncertainties) can be used as well. For instance overapproximation techniques based on the Jordan normal form approach (JNF) [12], on the Cayley–Hamilton theorem (CH) [26], and on Taylor series [7], can be employed in a similar fashion. However, according to [27], the GNB method seems to be the most favorable of these four techniques considering both numerical complexity and accuracy. Moreover, Procedure 1 can be extended to make it an automated procedure that iteratively refines the overapproximation (by adding additional grid points where necessary), yielding an overapproximation that is arbitrarily tight in an appropriate sense. For the sake of brevity, we do not discuss this extension and refer to [2, Procedure III.1] for the details on this extension. However, in the example section below, we briefly illustrate the functionality of this refinement procedure.

4. Input-to-state and ℓ_2-stability of switched systems with parametric uncertainty

In the previous sections, we obtained a switched discrete-time uncertain NCS model (10) and introduced an overapproximation technique to embed system (10) in a switched polytopic system with norm-bounded uncertainty as in (26), satisfying (28). In this section, we will employ this overapproximated system to develop conditions that guarantee EISS and an upper bound on the ℓ_2-gain, given a particular protocol and a set Θ as in (5). In the following lemmas, we state general sufficient conditions in terms of dissipation inequalities that guarantee EISS and an upper bound on the ℓ_2-gain.

Lemma 3. *Consider the system* (26) *with switching function* (12) *or* (17) *and uncertainty set* $\boldsymbol{\Delta}$ *as in* (31). *Suppose there exist some positive scalars* $\alpha_1, \alpha_2, \alpha_3, \kappa$ *and a function* $V : \mathbb{R}^{n_x} \times \mathbb{N} \to \mathbb{R}^{n_x}$ *such that*

$$\alpha_1 \|\bar{x}_k\|^2 \leqslant V(\bar{x}_k, k) \leqslant \alpha_2 \|\bar{x}_k\|^2 \tag{32a}$$

$$V(\bar{x}_{k+1}, k+1) - V(\bar{x}_k, k) \leqslant -\alpha_3 \|\bar{x}_k\|^2 + \kappa \|\bar{\epsilon}_k\|^2 \tag{32b}$$

for all $\bar{x}_k \in \mathbb{R}^{n_x}, \bar{\epsilon}_k \in \mathbb{R}^{n_z}$ *and all* $k \in \mathbb{N}$, *with* $\bar{x}_{k+1}$ *given by* (26) *for some* $\alpha_k \in \mathcal{A}$ *and some* $\Delta_k \in \boldsymbol{\Delta}$. *Then, the system* (26) *is EISS with respect to bounded disturbances with* $c = \sqrt{\frac{\alpha_2}{\alpha_1}}, \lambda = \sqrt{1 - \frac{\alpha_3}{\alpha_2}} \in [0, 1)$ *and ISS-gain*

$$\gamma_{ISS} = \sqrt{\frac{\alpha_2 \kappa}{\alpha_1 \alpha_3}}. \tag{33}$$

A function that satisfies (32) *is called an EISS-Lyapunov function.*

Proof. The proof follows from Theorem 2.5 of [28], adopted for linear gains. $\square$

Lemma 4. *Consider the system* (26) *with switching function* (12) *or* (17) *and uncertainty set* $\boldsymbol{\Delta}$ *as in* (31). *Suppose there exist some positive scalars* $\alpha_1, \alpha_2, \alpha_4, \kappa$ *and a storage function* $V : \mathbb{R}^{n_x} \times \mathbb{N} \to \mathbb{R}^{n_x}$ *such that*

$$\alpha_1 \|\bar{x}_k\|^2 \leqslant V(\bar{x}_k, k) \leqslant \alpha_2 \|\bar{x}_k\|^2 \tag{34a}$$

$$V(\bar{x}_{k+1}, k+1) - V(\bar{x}_k, k) \leqslant \kappa \|\bar{\epsilon}_k\|^2 - \alpha_4 \|\bar{z}_k\|^2 \tag{34b}$$

for all $\bar{x}_k \in \mathbb{R}^{n_x}, \bar{z}_k, \bar{\epsilon}_k \in \mathbb{R}^{n_z}$ *and all* $k \in \mathbb{N}$, *with* $\bar{x}_{k+1}$ *given by* (26) *for some* $\alpha_k \in \mathcal{A}$ *and some* $\Delta_k \in \boldsymbol{\Delta}$. *Then, the system* (26) *has an* ℓ_2-*gain smaller than or equal to*

$$\gamma_{\ell_2} = \sqrt{\frac{\kappa}{\alpha_4}}. \tag{35}$$

Proof. The proof is given in Appendix A. $\square$

Lemmas 3 and 4 will be used to prove the main results that we will present below. The proof of these results will be based on the existence of a function V that satisfies the following inequality constraint

$$V(\bar{x}_{k+1}, k+1) - V(\bar{x}_k, k) \leqslant -\alpha_3 \|\bar{x}_k\|^2 - \alpha_4 \|\bar{z}_k\|^2 + \kappa \|\bar{\epsilon}_k\|^2, \tag{36}$$

for some $\alpha_3, \alpha_4, \kappa > 0$, as this expression simultaneously implies both (32b) and (34b).

In the next section, we will provide sufficient conditions in terms of LMIs under which system (26), and thus the NCS model (10) (due to (28)), with a given quadratic or periodic protocol, is EISS and has an upper bound on the ℓ_2-gain. To do so, let us introduce the set of matrices $\mathcal{R}$ given by

$$\mathcal{R} = \{\text{diag}(r_1 I_1, \ldots, r_K I_K, r_{K+1} I_1, \ldots, r_{2K} I_K, r_{2K+1} I_1, \ldots, r_{3K} I_K) \mid r_i > 0 \text{ for } i \in \{1, \ldots, 3K\}\}, \tag{37}$$

where $I_i \in \mathbb{R}^{n_i \times n_i}$ is an identity matrix of the size of the i-th real Jordan block $\Lambda_i, i \in \{1, \ldots, K\}$, of $\bar{\Lambda}$.

4.1. Quadratic protocols

We will now analyze EISS and the ℓ_2-gain for the system (10) with protocol (12). Therefore, let us introduce a candidate EISS-Lyapunov function/ℓ_2-gain storage function of the form

$$V(\bar{x}_k, k) = \bar{x}_k^\top P_i \bar{x}_k, \tag{38}$$

in which $i = \min\{j \in \{1, \ldots, N\} \mid x \in \Omega_j\}$ and where the set Ω_j is given by

$$\Omega_j = \left\{ \begin{bmatrix} \bar{x} \\ \bar{\epsilon} \end{bmatrix} \in \mathbb{R}^{n_x + n_z} \ \middle| \ \begin{bmatrix} \bar{x} \\ \bar{\epsilon} \end{bmatrix}^\top Q_j \begin{bmatrix} \bar{x} \\ \bar{\epsilon} \end{bmatrix} \leqslant \begin{bmatrix} \bar{x} \\ \bar{\epsilon} \end{bmatrix}^\top Q_f \begin{bmatrix} \bar{x} \\ \bar{\epsilon} \end{bmatrix} \text{ for all } f \in \{1, \ldots, N\} \right\}. \tag{39}$$

Theorem 5. *Assume that there exist positive definite matrices* $P_i, i \in \{1, \ldots, N\}$, *matrices* $R_{i,l} \in \mathcal{R}, i \in \{1, \ldots, N\}$ *and* $l \in \{1, \ldots, L\}$, *positive scalars* $\alpha_3, \alpha_4, \kappa$, *non-negative scalars* $\xi_{i,f}, i, f \in \{1, \ldots, N\}$, *satisfying*

$$\begin{bmatrix} P_i + \bar{Q}_{11}^i & \bar{Q}_{12}^i & 0 & \bar{A}_{i,l}^\top P_j & \bar{C}_i^\top R_{i,l} & \alpha_3 I & \alpha_4 \tilde{H}_i^\top \\ \star & \kappa I + \bar{Q}_{22}^i & 0 & \bar{E}_{i,l}^\top P_j & \bar{F}_i^\top R_{i,l} & 0 & 0 \\ \star & \star & R_{i,l} & \bar{B}^\top P_j & 0 & 0 & 0 \\ \star & \star & \star & P_j & 0 & 0 & 0 \\ \star & \star & \star & \star & R_{i,l} & 0 & 0 \\ \star & \star & \star & \star & \star & \alpha_3 I & 0 \\ \star & \star & \star & \star & \star & \star & \alpha_4 I \end{bmatrix} \succeq 0 \tag{40}$$

for all $i \in \{1, \ldots, N\}$, $l \in \{1, \ldots, L\}$ with $\bar{Q}_{11}^i := \sum_{f=1}^N \xi_{i,f}(Q_{11}^i - Q_{11}^f)$, $\bar{Q}_{12}^i := \bar{Q}_{21}^{i\top} := \sum_{f=1}^N \xi_{i,f}(Q_{12}^i - Q_{12}^f)$ and $\bar{Q}_{22}^i := \sum_{f=1}^N \xi_{i,f}(Q_{22}^i - Q_{22}^f)$. Then, the system (10) with protocol (12), with matrices Q_{11}^i, Q_{12}^i and Q_{22}^i, $i \in \{1, \ldots, N\}$, given by (13), is EISS with an upper bound on the ISS-gain γ_{ISS} given by (33), in which $\alpha_1 = \min_{i \in \{1, \ldots, N\}} \lambda_{\min}(P_i)$ and $\alpha_2 = \max_{i \in \{1, \ldots, N\}} \lambda_{\max}(P_i)$, and has an ℓ_2-gain γ_{ℓ_2} smaller than or equal to (35).

Proof. The proof is given in the Appendix. □

4.2. Periodic protocols

We will now analyze EISS and ℓ_2-gain properties of the system (10) for the class of periodic protocols (17). Let us introduce positive definite matrices P_i, $i \in \{1, \ldots, \tilde{N}\}$, and a time-dependent periodic candidate EISS-Lyapunov function/ℓ_2-gain storage function, for $k \in \mathbb{N}$, of the form

$$V(\bar{x}_k, k) = \bar{x}_k^\top P_{k \bmod \tilde{N}} \bar{x}_k, \tag{41}$$

where $k \bmod \tilde{N}$ denotes k modulo $\tilde{N}$, which is the remainder of the division of k by $\tilde{N}$.

Theorem 6. *Assume that there exist positive definite matrices P_i, $i \in \{1, \ldots, \tilde{N}\}$, matrices $R_{i,l} \in \mathcal{R}$, $i \in \{1, \ldots, \tilde{N}\}$ and $l \in \{1, \ldots, L\}$, and positive scalars α_3, α_4, κ, satisfying*

$$\begin{bmatrix} P_i & 0 & 0 & \bar{A}_{\sigma_i,l}^\top P_{i+1} & \bar{C}_{\sigma_i}^\top R_{i,l} & \alpha_3 I & \alpha_4 \tilde{H}_{\sigma_i}^\top \\ \star & \kappa I & 0 & \bar{E}_{\sigma_i,l}^\top P_{i+1} & \bar{F}_{\sigma_i}^\top R_{i,l} & 0 & 0 \\ \star & \star & R_{i,l} & \bar{B}^\top P_{i+1} & 0 & 0 & 0 \\ \star & \star & \star & P_{i+1} & 0 & 0 & 0 \\ \star & \star & \star & \star & R_{i,l} & 0 & 0 \\ \star & \star & \star & \star & \star & \alpha_3 I & 0 \\ \star & \star & \star & \star & \star & \star & \alpha_4 I \end{bmatrix} \succeq 0, \tag{42}$$

where $P_{\tilde{N}+1} := P_1$, for all $i \in \{1, \ldots, \tilde{N}\}$, $l \in \{1, \ldots, L\}$. Then, the system (10) with protocol (17), is EISS with an upper bound on the ISS-gain γ_{ISS} given by (33), in which $\alpha_1 = \min_{i \in \{1, \ldots, \tilde{N}\}} \lambda_{\min}(P_i)$ and $\alpha_2 = \max_{i \in \{1, \ldots, \tilde{N}\}} \lambda_{\max}(P_i)$, and has an ℓ_2-gain γ_{ℓ_2} smaller than or equal to (35).

Proof. The proof follows the same lines of reasoning as the proof of Theorem 5 and is therefore omitted. □

5. Stability conditions for different quantizers

In the previous section, we derived conditions for guaranteeing EISS and an upper bound on the ℓ_2-gain of the switched discrete-time uncertain system (10) and protocols (12) or (17) in terms of LMIs. With these results, we can formulate stability conditions for the NCS with both types of quantizers (uniform and logarithmic quantizers) discussed in Section 2.3.

5.1. Uniform quantizer

The bound on the quantization-induced disturbance of the i-th component of $\bar{\epsilon}_k$, given a uniform quantizer, is given by (20). Using the fact that $\|\bar{\epsilon}_k\|^2 = \sum_{i=1}^{n_z} |\bar{\epsilon}_k^i|^2$, we arrive at a bound on $\bar{\epsilon}_k$ given by $\|\bar{\epsilon}_k\| \leqslant \sqrt{\sum_{i=1}^{n_z} \left(\frac{\zeta_i}{2}\right)^2}$. Using both this bound on $\bar{\epsilon}_k$ and assuming EISS of (10) as in Definition 1 (which can be verified by using the conditions in Theorem 5 or Theorem 6), we arrive at an ultimate bound (UB) for the solutions $\bar{x}_k$ of (10) as $k \to \infty$, given by

$$\limsup_{k \to \infty} \|\bar{x}_k\| \leqslant \gamma_{ISS} \sup_{s \in \mathbb{N}} \|\bar{\epsilon}_s\| \leqslant \gamma_{ISS} \sqrt{\sum_{i=1}^{n_z} \left(\frac{\zeta_i}{2}\right)^2}, \tag{43}$$

that depends on both the ISS-gain γ_{ISS} as well as the quantization density of all input/output signals, where the ISS gain γ_{ISS} can be expressed as follows

$$\gamma_{ISS} = \sqrt{\frac{\max_{i \in \{1, \ldots, N\}} \lambda_{\max}(P_i) \kappa}{\min_{i \in \{1, \ldots, N\}} \lambda_{\min}(P_i) \alpha_3}}, \tag{44}$$

in which α_3, $\kappa > 0$ and $P_i > 0$, $i = 1, 2, \ldots, N$, satisfy the conditions of Theorem 5 or Theorem 6.

As indicated by (43), practical stability of the system (10) is achieved with respect to the quantization step-size ζ_i, $i \in \{1, \ldots, n_z\}$, since it holds that selecting $\zeta_i \to 0$, for all $i \in \{1, \ldots, n_z\}$, implies that $\limsup_{k \to \infty} \|\bar{x}_k\| \to 0$. However, for

any fixed ζ_i, the solutions $\bar{x}_k$ to system (10) have a certain UB. To obtain the smallest upper bound on the UB in (43), we aim at minimizing γ_{ISS} subject to the LMIs (40) or (42), with free variables P_i, and positive scalars α_3 and κ. Hence, we take $\alpha_4 = 0$ in (40) or (42), since we are not interested in the ℓ_2-gain. Note that, minimizing the γ_{ISS} is a nonlinear minimization problem, which is in general not straightforward to solve. However, one efficient technique to solve this problem is discussed next.

Minimizing the upper bound on the ISS gain of the system (10), with protocols (12) or (17) is achieved by fixing $\alpha_3 > 0$, and putting a bound on both $\max_{i\in\{1,\dots,N\}} \lambda_{\max}(P_i)$ and $\min_{i\in\{1,\dots,N\}} \lambda_{\min}(P_i)$, by using the additional constraints $\underline{\omega}I \leqslant P_i \leqslant \overline{\omega}I$, for some $\underline{\omega}, \overline{\omega} > 0$. Consequently, we have $\alpha_1 = \min_{i\in\{1,\dots,N\}} \lambda_{\min}(P_i) \geqslant \underline{\omega}$ and $\alpha_2 = \max_{i\in\{1,\dots,N\}} \lambda_{\max}(P_i) \leqslant \overline{\omega}$, for all $i \in \{1, \dots, N\}$ using protocol (12) and $i \in \{1, \dots, \tilde{N}\}$ for protocol (17). Subsequently, we minimize over κ.

5.2. Logarithmic quantizer

The quantization-induced disturbance of the i-th component of $\bar{\epsilon}_k$ using a logarithmic quantizer is given by (23), and is directly related to the quantization density η_i, $i \in \{1, \dots, n_z\}$, for each input/output signal. Using the Euclidean norm, we arrive at a bound on $\bar{\epsilon}_k$ given by $\|\bar{\epsilon}_k\|^2 \leqslant \max_{i\in\{1,\dots,n_z\}} \delta_i^2 \|\bar{z}_k\|^2$. Using this bound in (36) results in

$$V(\bar{x}_{k+1}, k+1) - V(\bar{x}_k, k) \leqslant -\alpha_3 \|\bar{x}_k\|^2 + (\kappa \bar{\delta}^2 - \alpha_4)\|\bar{z}_k\|^2, \tag{45}$$

in which we defined $\bar{\delta} := \max_{i\in\{1,\dots,n_z\}} \delta_i$. In order to achieve global exponential stability (GES), we require that $(\kappa \bar{\delta}^2 - \alpha_4) \leqslant 0$. Therefore, we have that $\bar{\delta} \leqslant \sqrt{\frac{\alpha_4}{\kappa}}$, which is the inverse of the upper bound on the ℓ_2-gain (35), i.e., $\gamma_{\ell_2}^{-1}$. As a result, the absolute minimum required quantization density for all input/output signals in order to obtain GES is given by $\eta_i \geqslant \frac{1-\gamma_{\ell_2}^{-1}}{1+\gamma_{\ell_2}^{-1}}$, $i = \{1, \dots, n_z\}$. Consequently, it is of interest to minimize the upper bound on the ℓ_2-gain (35) as this yields the coarsest logarithmic quantizers that still guarantee GES of the NCS.

Remark 5. The modeling and analysis framework presented in this paper also allows to include another class of quantizers, namely, 'zoom quantizers', as introduced in [18]. Namely, under the assumption that all quantizers have an infinite range, there exists a bound on the quantization error. This guarantees that the zoom quantizer is allowed to 'zoom in' continuously, thereby guaranteeing that the quantization error dynamics to be GES. This allows us to guarantee GES of the NCS, provided that the system (10) is EISS. This is due to the fact that a cascade of a GES system (describing the quantization error dynamics) with an EISS system (being system (10)) is guaranteed to be GES.

Remark 6. Note that using system (10) with (12) or (17), we can only prove the above stability properties at the transmission instants, while the states of (1) actually also evolve continuously between these transmission times. However, by using conditions presented in [29], we can show that obtaining an upper bound on the UB for system (10) in the case of a uniform quantizer or proving GES of system (10) in the case of a logarithmic quantizer implies that the continuous-time NCS has an upper bound on the UB or is GES as well. Essentially, this can be done by showing that the intersample behavior is bounded as function of the norms of the states at the transmission instants. However, for the sake of brevity, we will not formally establish this result.

6. Illustrative example

In this section, we illustrate the presented theory using a well-known benchmark example in the NCS literature, see, e.g., [3,24], consisting of a linearized model of a batch reactor controlled by a continuous-time proportional and integral controller. We refer to the aforementioned references for details regarding the linearized model as well as the controller. Furthermore, the numerical results in this section are obtained by using a Matlab NCS Toolbox, which is currently being developed and is discussed in [30].

As in [3,24], we assume that the controller is given in continuous-time and directly connected to the actuators. Hence, only the two plant outputs are communicated via a network and $n_z = n_y = 2$. As already indicated in Remark 4, this requires slight modifications of the matrices (11). The fact that only two plant outputs are communicated over a shared network leads to the construction of two sensor nodes, $N = 2$, where the first node contains plant output y_1 and the second node contains y_2, i.e., $\Gamma_1 = \text{diag}(1, 0)$ and $\Gamma_2 = \text{diag}(0, 1)$. Furthermore, we assume that dropouts do not occur in this example, although they could easily be accommodated for as indicated in Remark 3. The lower bounds on the transmission intervals and delays are selected as $\underline{h} = 10^{-3}$ and $\underline{\tau} = 10^{-3}$, respectively. Both upper bounds $\bar{h}$ and $\bar{\tau}$ on the transmission intervals and delays are left open, where the NCS toolbox [30] employs an optimization algorithm to determine Pareto optimal values for $\bar{h}$ and $\bar{\tau}$, using the LMIs in Theorems 5 and 6. Hereto, a convex overapproximation of the NCS model (10) is required. We use the GNB overapproximation technique, as already implemented in the NCS toolbox [30], i.e., we employ Procedure 1 in which we select the maximum number of grid points $L = 100$, to obtain an appropriate overapproximation of the NCS model (10) as in (26), satisfying (28). This procedure typically starts from a rough initial partitioning of Θ with a small number of grid points, which for instance, for the values of $\bar{h} = 0.045$ and $\bar{\tau} = 0.0245$, consists of the two triangles, as in (29), as indicated by the thick lines in Fig. 3. The automatic refinement method, as mentioned briefly in Section 3 and implemented in the
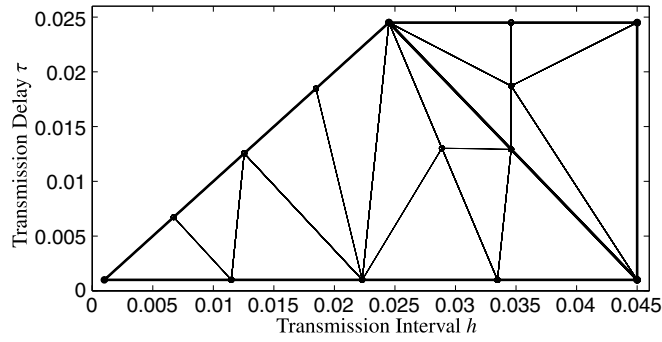
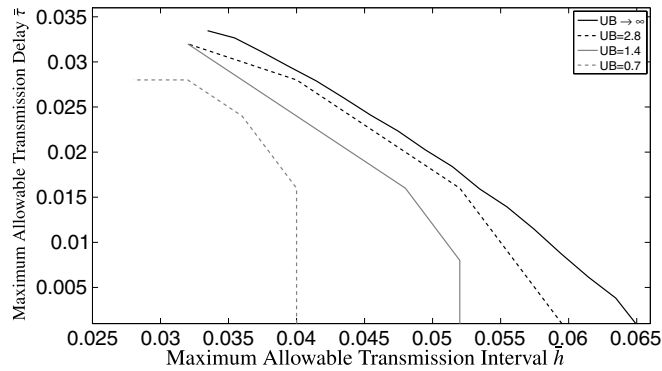**Fig. 3.** A typical subdivision of the set Θ into a set of triangles.

Fig. 4. Numerical results of minimization of γ_{ISS}, resulting in various upper bounds on the UB.
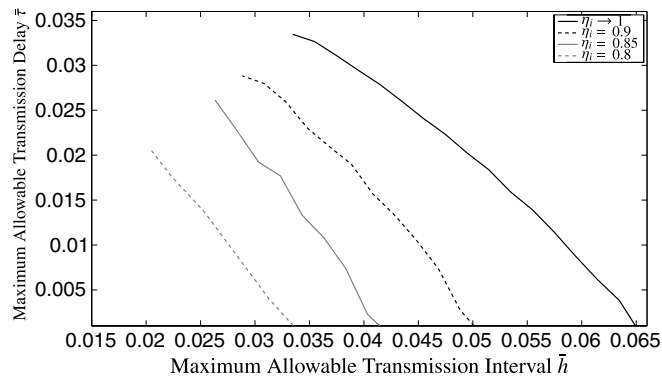

Fig. 5. Numerical results for the logarithmic quantizer.

NCS toolbox, includes new grid points and thus creates new triangles in order to minimize the size of the norm-bounded uncertainties in (26). This refinement procedure results after a few iterations in the partition of Θ as in Fig. 3. Following this procedure for various values of $\bar{h}$ and $\bar{\tau}$ for the quantization-free case, and verifying feasibility of the corresponding LMIs lead to a tradeoff curve, guaranteeing GES, as represented for the NCS with RR protocol by the solid black line in both Figs. 4 and 5. In the remainder of this example, we only present simulation results obtained for the RR protocol for the sake of brevity.

First we consider the case where both output signals are quantized using a uniform quantizer with step size $\zeta_i = 10^{-3}$, $i = 1, 2$. The objective is now to obtain the smallest upper bound on the UB (43) by minimizing the ISS-gain (33) of (10) as described in Section 5.1. Hereto, we exploit the convex overapproximation of (10) and check for numerous combinations of $\bar{h}$ and $\bar{\tau}$ whether the LMIs of Theorem 6 are feasible, while minimizing γ_{ISS}. This provides information on an upper bound on γ_{ISS} depending on the bounds $\bar{h}$ and $\bar{\tau}$ on the transmission intervals and delays, respectively. Using this information in (43), together with the quantization step sizes of both plant outputs ζ_i, $i = 1, 2$, we can compute an upper bound on the UB on the states. The results for this example are depicted in Fig. 4, where we selected $\alpha_3 = 10^{-3}$, $\underline{\omega} = 10^{-1}$ and $\bar{\omega} = 50$. The non-quantized curve forms a boundary for an NCS with uniform quantizer as beyond this boundary, we cannot guarantee

a finite UB. Notice that the gradient of the UB becomes steeper the closer we approach the curve for UB $\to \infty$. This means that, for this example, we can have a significantly smaller upper bound on the UB by allowing only a slight reduction in $\bar{h}$ and/or $\bar{\tau}$.

For the NCS with a logarithmic quantizer, the ℓ_2-gain of (10) is directly related to the minimum required quantization density η_i, $i = 1, 2$, for all plant output signals. We obtain tradeoff curves as a function of this quantization density, guaranteeing GES of (10), by selecting these η_i and, thereby, fixing the ℓ_2-gain. Subsequently, we use the convex overapproximation of (10) to check for a grid in both $\bar{h}$ and $\bar{\tau}$ whether the LMIs (42) are feasible. The results for a numerical analysis are depicted in Fig. 5, where we selected $\alpha_3 = 10^{-10}, \alpha_4 = 10^{-3}$ and chose $\kappa = \alpha_4 \frac{(1+\eta_i)^2}{(1-\eta_i)^2}$ for three distinct values of η_i, which are selected equal in this example for both output signals, i.e., $\eta_i = 0.8$, $\eta_i = 0.85$ and $\eta_i = 0.9$, $i = 1, 2$. As in Fig. 4, the solid black line represents the non-quantized tradeoff curve, as it requires infinitely dense quantization steps ($\eta_i \to 1, i = 1, 2$) to reach this curve. From Fig. 5 it can be observed that a denser quantizer is required as we approach the non-quantized curve more closely.

7. Conclusions

In this paper, we analyzed the stability of networked control systems (NCSs) that are subject to quantization effects, time-varying transmission intervals, time-varying delays and communication constraints and discussed how dropouts could be included as well. The analysis is performed using a comprehensive modeling framework for NCSs based on discrete-time switched linear uncertain systems. To handle the exponential uncertainty in the system matrices caused by the presence of varying transmission intervals and delays, a procedure that yields a convex overapproximation has been used and extended. Exploiting the resulting overapproximated systems, we derived LMI-based conditions that guarantee exponential input-to-state stability (EISS) and ℓ_2-stability of the NCS and showed how these conditions can be used to compute an ultimate bound on the state for uniform quantizers, and to prove global exponential stability (GES) for logarithmic quantizers. The application of the newly derived theory to a benchmark example showed that the developed theory can be used to make tradeoffs between the various network properties, such as bounds on transmission intervals and delays, the quantization properties and control criteria, such as ultimate bounds (in case of uniform quantizers) and GES (in case of logarithmic quantizers). Consequently, this work provides designers of NCSs with new and computationally efficient tools to support their multi-disciplinary design choices.

Acknowledgments

Appendix A. Proof of Lemma 4

Since the storage function V satisfies (34), we have for any $n \in \mathbb{N}$ that

$$\sum_{k=0}^{n} (V(\bar{x}_{k+1}, k+1) - V(\bar{x}_k, k)) \leqslant \sum_{k=0}^{n} \left(\kappa \bar{\epsilon}_k^\top \bar{\epsilon}_k - \alpha_4 \bar{z}_k^\top \bar{z}_k \right), \tag{A.1}$$

which is equivalent to

$$0 \leq V(\bar{x}_{n+1}, n+1) \leqslant \sum_{k=0}^{n} \kappa \|\bar{\epsilon}_k\|^2 - \sum_{k=0}^{n} \alpha_4 \|\bar{z}_k\|^2 + V(\bar{x}_0). \tag{A.2}$$

Now letting $n \to \infty$, we have

$$\|\bar{z}_k\|_{\ell_2} \leqslant \sqrt{\frac{\kappa}{\alpha_4}} \|\bar{\epsilon}_k\|_{\ell_2} + \sqrt{\frac{1}{\alpha_4} V(\bar{x}_0)}, \tag{A.3}$$

where we used the inequality $\sqrt{a+b} \leqslant \sqrt{a} + \sqrt{b}$, for $a, b > 0$, which satisfies (25) with $\gamma_{\ell_2} = \sqrt{\frac{\kappa}{\alpha_4}}$, for all disturbances for which $\sum_{k=0}^{\infty} \|\bar{\epsilon}_k\|^2$ is finite.

Appendix B. Proof of Theorem 5

The proof is based on showing that (38) is both an EISS-Lyapunov function as well as an ℓ_2-gain storage function for the discrete-time switched uncertain system (10) with protocol (12). As a consequence, (38) should fulfill the hypotheses of Lemmas 3 and 4. Due to positive definiteness of the matrices P_i, $i \in \{1, \ldots, N\}$, conditions (32a) and (34a) are satisfied with $\alpha_1 = \min_{i \in \{1, \ldots, N\}} \lambda_{\min}(P_i)$ and $\alpha_2 = \max_{i \in \{1, \ldots, N\}} \lambda_{\max}(P_i)$. Hence, it remains to show that V as in (38) fulfills (36) if the conditions in the theorem are satisfied, for all $[\bar{x}_k^\top \ \bar{\epsilon}_k^\top]^\top \in \Omega_i$, $i \in \{1, \ldots, N\}$, and $\bar{x}_{k+1} \in \mathbb{R}^{n_x}$, $\bar{z}_k, \bar{\epsilon}_k \in \mathbb{R}^{n_z}$ and some scalars $\alpha_3, \alpha_4, \kappa > 0$. Since, for all $[\bar{x}_k^\top \ \bar{\epsilon}_k^\top]^\top \in \Omega_i$, it holds that $\begin{bmatrix} \bar{x}_k \\ \bar{\epsilon}_k \end{bmatrix}^\top (Q_i - Q_f) \begin{bmatrix} \bar{x}_k \\ \bar{\epsilon}_k \end{bmatrix} \leqslant 0, f \in \{1, \ldots, N\}$, we have that (36) is satisfied if there exists $\xi_{i,f} \geqslant 0$, such that

$$\bar{x}_{k+1}^\top P_j \bar{x}_{k+1} - \bar{x}_k^\top P_i \bar{x}_k \leqslant -\alpha_3 \bar{x}_k^\top \bar{x}_k - \alpha_4 \bar{x}_k^\top \tilde{H}_i^\top \tilde{H}_i \bar{x}_k + \kappa \bar{\epsilon}_k^\top \bar{\epsilon}_k + \sum_{f=1}^N \xi_{i,f} \begin{bmatrix} \bar{x}_k \\ \bar{\epsilon}_k \end{bmatrix}^\top (Q_i - Q_f) \begin{bmatrix} \bar{x}_k \\ \bar{\epsilon}_k \end{bmatrix}, \tag{B.1}$$

or equivalently

$$\left(\tilde{A}_{\sigma_k, h_k, \tau_k} \bar{x}_k + \tilde{B}_{\sigma_k, h_k, \tau_k} \bar{\epsilon}_k \right)^\top P_j \left(\tilde{A}_{\sigma_k, h_k, \tau_k} \bar{x}_k + \tilde{B}_{\sigma_k, h_k, \tau_k} \bar{\epsilon}_k \right) - \bar{x}_k^\top P_i \bar{x}_k$$

$$\leqslant -\alpha_3 \bar{x}_k^\top \bar{x}_k - \alpha_4 \bar{x}_k^\top \tilde{H}_i^\top \tilde{H}_i \bar{x}_k + \kappa \bar{\epsilon}_k^\top \bar{\epsilon}_k + \sum_{f=1}^N \xi_{i,f} \begin{bmatrix} \bar{x}_k \\ \bar{\epsilon}_k \end{bmatrix}^\top (Q_i - Q_f) \begin{bmatrix} \bar{x}_k \\ \bar{\epsilon}_k \end{bmatrix}, \tag{B.2}$$

for all $j \in \{1, \ldots, N\}$. Because (26) is an overapproximation of (10) in the sense of (28), we have that (B.2) is implied by

$$\begin{bmatrix} \bar{x} \\ \bar{\epsilon} \end{bmatrix}^\top \underbrace{\begin{bmatrix} \Xi_{11} & \Xi_{12} \\ \star & \Xi_{22} \end{bmatrix}}_{=: \bar{\Xi}} \begin{bmatrix} \bar{x} \\ \bar{\epsilon} \end{bmatrix} \leqslant 0, \tag{B.3}$$

in which

$$\Xi_{11} := \left(\sum_{l_1=1}^L \alpha^{l_1} \bar{A}_{i,l_1} + \bar{B} \Delta \bar{C}_i \right)^\top P_j \left(\sum_{l_2=1}^L \alpha^{l_2} \bar{A}_{i,l_2} + \bar{B} \Delta \bar{C}_i \right) - P_i - \bar{Q}_{11}^i + \alpha_3 I + \alpha_4 \tilde{H}_i^\top \tilde{H}_i,$$

$$\Xi_{12} := \left(\sum_{l_1=1}^L \alpha^{l_1} \bar{A}_{i,l_1} + \bar{B} \Delta \bar{C}_i \right)^\top P_j \left(\sum_{l_2=1}^L \alpha^{l_2} \bar{E}_{i,l_2} + \bar{B} \Delta \bar{F}_i \right) - \bar{Q}_{12}^i,$$

$$\Xi_{22} := \left(\sum_{l_1=1}^L \alpha^{l_1} \bar{E}_{i,l_1} + \bar{B} \Delta \bar{F}_i \right)^\top P_j \left(\sum_{l_2=1}^L \alpha^{l_2} \bar{E}_{i,l_2} + \bar{B} \Delta \bar{F}_i \right) - \kappa I - \bar{Q}_{22}^i,$$

for all $\alpha \in \mathcal{A}$, $\Delta \in \boldsymbol{\Delta}$ and $\alpha_3, \alpha_4, \kappa > 0$, where the matrices $\bar{Q}_{11}^i$, $\bar{Q}_{12}^i$ and $\bar{Q}_{22}^i$ are defined in the theorem. The inequality in (B.3) is equivalent to requiring that $\bar{\Xi} \preceq 0$, for all $\alpha \in \mathcal{A}$, $\Delta \in \boldsymbol{\Delta}$ and $i \in \{1, \ldots, N\}$. By taking a Schur complement, realizing that $P_j \succ 0$ for all $j \in \{1, \ldots, N\}$, and using that $\alpha \in \mathcal{A}$, we obtain that $\bar{\Xi} \preceq 0$ is equivalent to $\sum_{l=1}^L \alpha^l G_{i,l} \succeq 0$ with

$$G_{i,l} = \begin{bmatrix} P_i + \bar{Q}_{11}^i - \alpha_3 I - \alpha_4 \tilde{H}_i^\top \tilde{H}_i & \bar{Q}_{12}^i & (\bar{A}_{i,l} + \bar{B} \Delta \bar{C}_i)^\top P_j \\ \star & \kappa I + \bar{Q}_{22}^i & (\bar{E}_{i,l} + \bar{B} \Delta \bar{F}_i)^\top P_j \\ \star & \star & P_j \end{bmatrix} \tag{B.4}$$

for all $\alpha \in \mathcal{A}$, $\Delta \in \boldsymbol{\Delta}$ and $i \in \{1, \ldots, N\}$. A necessary and sufficient condition for $\sum_{l=1}^L \alpha^l G_{i,l} \succeq 0$, for all $\alpha \in \mathcal{A}$ and $i \in \{1, \ldots, N\}$, is that $G_{i,l} \succeq 0$ for all $i \in \{1, \ldots, N\}$ and $l \in \{1, \ldots, L\}$. Now observe that for all $\Delta \in \boldsymbol{\Delta}$, it holds that $[\bar{C}_i \ \bar{F}_i]^\top (R_{i,l} - \Delta^\top R_{i,l} \Delta) [\bar{C}_i \ \bar{F}_i] \succeq 0$, for all $R_{i,l} \in \mathcal{R}$, $i \in \{1, \ldots, N\}$ and $l \in \{1, \ldots, L\}$. Hence, $G_{i,l} \succeq 0$ if

$$\begin{bmatrix} P_i + \bar{Q}_{11}^i - \alpha_3 I - \alpha_4 \tilde{H}_i^\top \tilde{H}_i & \bar{Q}_{12}^i & (\bar{A}_{i,l} + \bar{B} \Delta \bar{C}_i)^\top P_j \\ \star & \kappa I + \bar{Q}_{22}^i & (\bar{E}_{i,l} + \bar{B} \Delta \bar{F}_i)^\top P_j \\ \star & \star & P_j \end{bmatrix}$$

$$\succ \begin{bmatrix} \bar{C}_i^\top R_{i,l} \bar{C}_i - \bar{C}_i^\top \Delta^\top R_{i,l} \Delta \bar{C}_i & \bar{C}_i^\top R_{i,l} \bar{F}_i - \bar{C}_i^\top \Delta^\top R_{i,l} \Delta \bar{F}_i & 0 \\ \star & \bar{F}_i^\top R_{i,l} \bar{F}_i - \bar{F}_i^\top \Delta^\top R_{i,l} \Delta \bar{F}_i & 0 \\ \star & \star & 0 \end{bmatrix} \succeq 0, \tag{B.5}$$

or equivalently, if the following inequality (obtained after applying two successive Schur complements),

$$
\begin{bmatrix} I & 0 & 0 \\ 0 & I & 0 \\ \Delta\bar{C}_i & \Delta\bar{F}_i & 0 \\ 0 & 0 & I \\ -\bar{C}_i & -\bar{F}_i & 0 \\ -I & 0 & 0 \\ -\tilde{H}_i & 0 & 0 \end{bmatrix}^\top \begin{bmatrix} P_i + \bar{Q}_{11}^i & \bar{Q}_{12}^i & 0 & \bar{A}_{i,l}^\top P_j & \bar{C}_i^\top R_{i,l} & \alpha_3 I & \alpha_4 \tilde{H}_i^\top \\ \star & \kappa I + \bar{Q}_{22}^i & 0 & \bar{E}_{i,l}^\top P_j & \bar{F}_i^\top R_{i,l} & 0 & 0 \\ \star & \star & R_{i,l} & \bar{B}^\top P_j & 0 & 0 & 0 \\ \star & \star & \star & P_j & 0 & 0 & 0 \\ \star & \star & \star & \star & R_{i,l} & 0 & 0 \\ \star & \star & \star & \star & \star & \alpha_3 I & 0 \\ \star & \star & \star & \star & \star & \star & \alpha_4 I \end{bmatrix} \begin{bmatrix} I & 0 & 0 \\ 0 & I & 0 \\ \Delta\bar{C}_i & \Delta\bar{F}_i & 0 \\ 0 & 0 & I \\ -\bar{C}_i & -\bar{F}_i & 0 \\ -I & 0 & 0 \\ -\tilde{H}_i & 0 & 0 \end{bmatrix} \succeq 0 \tag{B.6}
$$

is verified. Note that (B.6) is satisfied by the satisfaction of (40) for all $i \in \{1, \ldots, N\}$ and $l \in \{1, \ldots, L\}$. Since (B.6) holds under the conditions in the theorem, we can conclude that both (32) and (34) are satisfied which proves that V as in (38) is an EISS-Lyapunov function and an ℓ_2-gain storage function. Consequently, this guarantees that (10) with protocol (12), is EISS with respect to $\bar{\epsilon}$, and has an upper bound on the ISS-gain γ_{ISS} given by (33), with $\alpha_1 = \min_{i \in \{1, \ldots, N\}} \lambda_{\min}(P_i)$ and $\alpha_2 = \max_{i \in \{1, \ldots, N\}} \lambda_{\max}(P_i)$, and has an ℓ_2-gain smaller than or equal to γ_{ℓ_2} in (35).

References

[1] N.W. Bauer, P.J.H. Maas, W.P.M.H. Heemels, Stability analysis of networked control systems: a sum of squares approach, Automatica 48 (8) (2012) 1514–1524.

[2] M.C.F. Donkers, W.P.M.H. Heemels, N. van de Wouw, L. Hetel, Stability analysis of networked control systems using a switched linear systems approach, IEEE Trans. Automat. Control 56 (9) (2011) 2101–2115.

[3] W.P.M.H. Heemels, A.R. Teel, N. van de Wouw, D. Nešić, Networked control systems with communication constraints: tradeoffs between transmission intervals, delays and performance, IEEE Trans. Automat. Control 55 (8) (2010) 1781–1796.

[4] H. Gao, T. Chen, J. Lam, A new delay system approach to network-based control, Automatica 44 (1) (2008) 39–52.

[5] R. Alur, A. D'Innocenzo, K.H. Johansson, G.J. Pappas, G. Weiss, Compositional modeling and analysis of multi-hop control networks, IEEE Trans. Automat. Control 56 (10) (2011) 2345–2357.

[6] D.J. Antunes, J.P. Hespanha, C.J. Silvestre, Stochastic hybrid systems with renewal transitions, in: American Control Conference, 2010, pp. 3124–3129.

[7] L. Hetel, J. Daafouz, C. Iung, Analysis and control of LTI and switched systems in digital loops via an event-based modelling, Internat. J. Control 81 (7) (2008) 1125–1138.

[8] P. Naghshtabrizi, J.P. Hespanha, A.R. Teel, Stability of delay impulsive systems with application to networked control systems, Trans. Inst. Meas. Control 32 (5) (2010) 511–528. Special Issue on Hybrid and Switched Systems.

[9] N. van de Wouw, P. Naghshtabrizi, M.B.G. Cloosterman, J.P. Hespanha, Tracking control for sampled-data systems with uncertain time-varying sampling intervals and delays, Int. J. Robust Nonlinear Control 20 (4) (2010) 387–411.

[10] L. Wu, J. Lam, X. Yao, J. Xiong, Robust guaranteed cost control of discrete-time networked control systems, Optim. Control Appl. Methods 32 (1) (2011) 95–112.

[11] D.J. Antunes, J.P. Hespanha, C.J. Silvestre, Volterra integral approach to impulsive renewal systems: application to networked control, IEEE Trans. Automat. Control 57 (3) (2012) 607–619.

[12] M.B.G. Cloosterman, L. Hetel, N. van de Wouw, W.P.M.H. Heemels, J. Daafouz, H. Nijmeijer, Controller synthesis for networked control systems, Automatica 46 (10) (2010) 1584–1594.

[13] N. van de Wouw, D. Nešić, W.P.M.H. Heemels, A discrete-time framework for stability analysis of nonlinear networked control systems, Automatica 48 (6) (2012) 1144–1153.

[14] D. Nešić, D. Liberzon, A unified framework for design and analysis of networked and quantized control systems, IEEE Trans. Automat. Control 54 (4) (2009) 732–747.

[15] W.P.M.H. Heemels, D. Nešić, A.R. Teel, N. van de Wouw, Networked and quantized control systems with communication delays, in: Joint 48th IEEE Conf. Decision and Control and 28th Chinese Control Conf., Shanghai, 2009, pp. 7929–7935.

[16] V. Suplin, E. Fridman, U. Shaked, Sampled-data $\mathcal{H}_\infty$ control and filtering: nonuniform uncertain sampling, Automatica 43 (6) (2007) 1072–1083.

[17] G.N. Nair, F. Fagnani, S. Zampieri, R.J. Evans, Feedback control under data rate constraints: an overview, Proc. IEEE 95 (1) (2007) 108–137.

[18] R. Brockett, D. Liberzon, Quantized feedback stabilization of linear systems, IEEE Trans. Automat. Control 45 (2000) 1279–1289.

[19] N. Elia, S.K. Mitter, Stabilization of linear systems with limited information, IEEE Trans. Automat. Control 46 (2001) 1384–1400.

[20] M. Fu, L. Xie, The sector bound approach to quantized feedback control, IEEE Trans. Automat. Control 50 (2005) 1698–1711.

[21] H. Gao, T. Chen, A new approach to quantized feedback control systems, Automatica 44 (2) (2008) 534–542.

[22] H. Ishii, B.A. Francis, Limited Data Rate in Control Systems with Networks: Lecture Notes in Control and Information Sciences, Vol. 275, Springer, Berlin, 2002.

[23] D. Delchamps, Stabilizing a linear system with quantized state feedback, IEEE Trans. Automat. Control 35 (8) (1990) 916–924.

[24] G. Walsh, H. Ye, L. Bushnell, Stability analysis of networked control systems, IEEE Trans. Control Syst. Technol. (2002) 438–446.

[25] Z.-P. Jiang, Y. Wang, Input-to-state stability for discrete-time nonlinear systems, Automatica 37 (6) (2001) 857–869.

[26] R.H. Gielen, S. Olaru, M. Lazar, W.P.M.H. Heemels, N. van de Wouw, S.I. Niculescu, On polytopic inclusions as a modeling framework for systems with time-varying delays, Automatica 46 (3) (2010) 615–619.

[27] W.P.M.H. Heemels, N. van de Wouw, R.H. Gielen, M.C.F. Donkers, L. Hetel, S. Olaru, M. Lazar, J. Daafouz, S.I. Niculescu, Comparison of overapproximation methods for stability analysis of networked control systems, in: Proc. Conf. Hybrid Systems: Computation and Control, 2010, pp. 181–190.

[28] M. Lazar, D. Muñoz de la Peña, W.P.M.H. Heemels, T. Alamo, On input-to-state stability of min–max nonlinear model predictive control, Systems Control Lett. 57 (2008) 39–48.

[29] D. Nešić, A.R. Teel, E.D. Sontag, Formulas relating $\mathcal{KL}$ stability estimates of discrete-time and sampled-data nonlinear systems, Systems Control Lett. (1999) 49–60.

[30] N.W. Bauer, S.J.L.M. van Loon, M.C.F. Donkers, N. van de Wouw, W.P.M.H. Heemels, Networked control systems toolbox: robust stability analysis made easy, in: 3rd IFAC Workshop on Distributed Estimation and Control in Networked Systems, 2012, pp. 55–60.

[31] S.J.L.M. van Loon, M.C.F. Donkers, N. van de Wouw, W.P.M.H. Heemels, Stability analysis of networked control systems with periodic protocols and uniform quantizers, in: 4th IFAC Conf. on Analysis and Design of Hybrid Systems, 2012, pp. 186–191.